JOC Article
pubs.acs.org/joc

Dialkynyl Carbene Derivatives: Generation and Characterization of Triplet *tert*-Butylpentadiynylidene (*t*-Bu−C≡C−C̈−C≡C−H) and Dimethylpentadiynylidene (Me−C≡C−C̈−C≡C−Me)

Phillip S. Thomas, Nathan P. Bowling, Nicola J. Burrmann, and Robert J. McMahon*

Department of Chemistry, University of Wisconsin, 1101 University Avenue, Madison, Wisconsin 53706

mcmahon@chem.wisc.edu

Received June 6, 2010

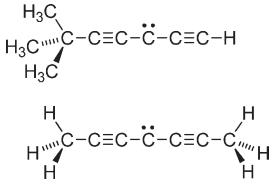

Triplet carbenes *t*-butylpentadiynylidene (*t*-BuC_5H, **1a**) and dimethylpentadiynylidene (MeC_5Me, **1b**) have been produced photochemically from their corresponding diazo compound precursors and studied spectroscopically in cryogenic matrices (N_2 or Ar) at 10 K. The infrared, electronic absorption, and electron paramagnetic resonance spectra of these species exhibit numerous similarities to the spectra of pentadiynylidene (HC_5H) and methylpentadiynylidene (MeC_5H) recorded previously. EPR spectra yield zero-field splitting parameters that are typical for triplet carbenes with axial symmetry (*t*-BuC_5H, **1a**: $|D/hc| = 0.61\ cm^{-1}$, $|E/hc| \sim 0\ cm^{-1}$; MeC_5Me, **1b**: $|D/hc| = 0.62\ cm^{-1}$, $|E/hc| \sim 0\ cm^{-1}$). Electronic spectra are characterized by weak absorptions ($T_1 \leftarrow T_0$) in the near-UV and visible region (350−430 nm) with extended vibronic progressions. The electronic transitions of several $-C_5-$ carbenes are compared, and an apparent dependence of the transition wavelength on the level of alkyl substitution of the carbon chain is found. Chemical trapping of triplet **1a** in an O_2-doped matrix affords carbonyl oxides derived predominantly from attack at C-3. Both *t*-BuC_5H (**1a**) and MeC_5Me (**1b**) undergo photochemical rearrangement upon UV irradiation.

Introduction

The chemistry and spectroscopy of carbon chain molecules are of significance in the fields of molecular spectroscopy,[1] combustion chemistry,[2,3] and astrochemistry.[4−7] Within the series of highly unsaturated carbon chain molecules HC_nH (n = odd), we recently focused our attention on the family of compounds containing a five-carbon chain ($R^1-C\equiv C-\ddot{C}-C\equiv C-R^2$).[8,9] These species are best envisioned as ground-state triplet dialkynyl carbenes, exhibiting characteristic spectroscopic signatures, particularly in their electronic[8,9] and EPR[10,11] spectra. The extensive unsaturation and delocalization present formidable challenges in the realm of electronic structure calculations.[12−16] Investigations of the electronic properties of these carbon chain

(1) Van Orden, A.; Saykally, R. J. *Chem. Rev*. **1998**, *98*, 2313–2357.
(2) Boullart, W.; Devriendt, K.; Borms, R.; Peeters, J. *J. Phys. Chem*. **1996**, *100*, 998–1007.
(3) Taatjes, C. A.; Klippenstein, S. J.; Hansen, N.; Miller, J. A.; Cool, T. A.; Wang, J.; Law, M. E.; Westmoreland, P. R. *Phys. Chem. Chem. Phys*. **2005**, *7*, 806–813.
(4) Kaiser, R. I. *Chem. Rev*. **2002**, *102*, 1309–1358.
(5) Herbst, E. *Chem. Soc. Rev*. **2001**, *30*, 168–176.
(6) Thaddeus, P.; McCarthy, M. C.; Travers, M. J.; Gottlieb, C. A.; Chen, W. *Faraday Discuss*. **1998**, *109*, 121–135.
(7) Hébrard, E.; Dobrijevic, M.; Bénilan, Y.; Raulin, F. *J. Photochem. Photobiol. C* **2007**, *7*, 211–230.
(8) Bowling, N. P.; Halter, R. J.; Hodges, J. A.; Seburg, R. A.; Thomas, P. S.; Simmons, C. S.; Stanton, J. F.; McMahon, R. J. *J. Am. Chem. Soc*. **2006**, *128*, 3291–3302.
(9) Thomas, P. S.; Bowling, N. P.; McMahon, R. J. *J. Am. Chem. Soc*. **2009**, *131*, 8649–8659.
(10) Bernheim, R. A.; Kempf, R. J.; Reichenbecher, E. F. *J. Magn. Reson*. **1970**, *3*, 5–9.
(11) Bernheim, R. A.; Kempf, R. J.; Gramas, J. V.; Skell, P. S. *J. Chem. Phys*. **1965**, *43*, 196–200.
(12) Fan, Q.; Pfeiffer, G. V. *Chem. Phys. Lett*. **1989**, *162*, 472–478.
(13) Seburg, R. A.; McMahon, R. J.; Stanton, J. F.; Gauss, J. *J. Am. Chem. Soc*. **1997**, *119*, 10838–10845.
(14) Horný, L.; Petraco, N. D. K.; Schaefer, H. F., III. *J. Am. Chem. Soc*. **2002**, *124*, 14716–14720.
(15) Mavrandonakis, A.; Mühlhäuser, M.; Froudakis, G. E.; Peyerimhoff, S. D. *Phys. Chem. Chem. Phys*. **2002**, *4*, 3318–3321.
(16) Zhang, C.; Cao, Z.; Wu, H.; Zhang, Q. *Int. J. Quantum Chem*. **2004**, *98*, 299–308.

Published on Web 09/02/2010 DOI: 10.1021/jo101096n

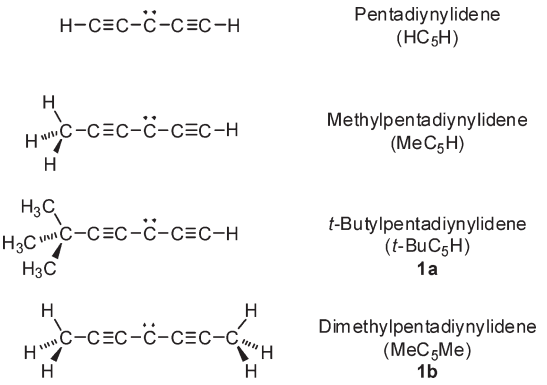

FIGURE 1. Triplet carbenes pentadiynylidene (HC_5H); methylpentadiynylidene (MeC_5H); *t*-butylpentadiynylidene (*t*-BuC_5H, **1a**), and dimethylpentadiynylidene (MeC_5Me, **1b**).

molecules may also provide insight concerning electrical conductivity at the molecular scale.[17,18] In terms of chemical reactivity, the $R^1-C_5-R^2$ carbenes dimerize to form enediynes,[8,19−21] which may undergo subsequent cycloaromatization reactions that could ultimately result in the formation of polycyclic aromatic hydrocarbons and soot.

In the current investigation, we describe the generation and characterization of triplet carbenes *t*-BuC_5H (**1a**) and MeC_5Me (**1b**) in cryogenic matrices. Photolysis of diazo compound precursors affords the carbenes, which are characterized by IR, UV/vis, and EPR spectroscopy. Both carbenes exhibit subsequent photochemistry. *t*-BuC_5H (**1a**) was trapped, chemically, by reaction with O_2. Vibronic spectral patterns and EPR zero-field splitting (ZFS) parameters of **1a** and **1b**, together with the data reported previously for HC_5H[8] and MeC_5H,[9] help establish trends for structure/property relationships within the $R^1-C_5-R^2$ family (Figure 1).

Background

Spectroscopic studies of the $R^1-C_5-R^2$ family of triplet carbenes date from the early 1960s. Bernheim, Skell, and coworkers obtained triplet EPR spectra of MeC_5H, *t*-BuC_5H, and PhC_5H in poly(chlorotrifluoroethylene) glasses at 77 K and determined the zero-field splitting (ZFS) parameters.[10,11] The magnitude of the dipolar coupling, D, is often interpreted as revealing the degree of delocalization of the unpaired spins—with a large D value reflecting the strong dipolar coupling in a localized triplet carbene. The D values for MeC_5H and *t*-BuC_5H ($|D/hc| = 0.61$ cm^{-1}) seemed surprisingly large,[10,11] by comparison to that of triplet methylene (0.69 cm^{-1}),[22] but this effect is now understood to occur as a consequence of the delocalization of *both* unpaired electrons, leading to large contributions to the dipolar coupling at each atom along the carbon backbone.[23,24] The very small E values ($|E/hc|$ = ca. 0 cm^{-1}) were interpreted in terms of axially symmetric structures for MeC_5H and *t*-BuC_5H.[10,11] At the time, these carbenes were depicted as penta-2,4-diyn-1-ylidene derivatives ($R^1-C\equiv C-C\equiv C-\ddot{C}-H$).[10,11] Subsequent investigations concerning the electronic structure of related species (R^1 = H or Me), however, support a penta-1,4-diyn-3-ylidene structure ($R^1-C\equiv C-\ddot{C}-C\equiv C-H$) as the dominant contributor to the resonance hybrid.[8,9] Iwamura and co-workers obtained the EPR spectrum of PhC_5Ph, which is believed to attain a linear $-C_5-$ backbone upon annealing the 2-methyltetrahydrofuran glass to 81 K.[25] Detailed interpretations of the temperature-dependent EPR spectra of phenyl-substituted $-C_3-$ and $-C_5-$ carbenes are complicated by conformation effects associated with the phenyl substituents.[8,26,27]

Maier and co-workers reported the electronic absorption spectra for individual members of the carbene series $HC_{2n+1}H$ (n = 2−7) in neon at 5 K.[28] The spectra of HC_7H, HC_9H, $HC_{11}H$, and $HC_{13}H$ displayed excellent signal-to-noise ratios, but that of HC_5H exhibited considerably lower intensity and was possibly contaminated by other species. Using the matrix data for triplet HC_5H as a guide, Ball et al. attempted to obtain a high-resolution gas-phase spectrum of HC_5H using cavity ring-down spectroscopy.[29] Despite exhaustive efforts, however, this species eluded observation. With the successful synthesis of 1-diazo-2,4-pentadiyne, a new photochemical precursor of HC_5H, we were finally able to characterize the carbene by IR, UV/visible, and EPR spectroscopy and by chemical trapping with molecular oxygen.[8] A subsequent investigation focused on the generation and characterization of triplet MeC_5H.[9]

Results and Discussion

Carbene Precursors. The protocol for generating carbenes *t*-BuC_5H (**1a**) and MeC_5Me (**1b**) begins with the synthesis of their corresponding tosylhydrazone precursors (**2a**, **2b**), as described elsewhere.[30] Treatment of the tosylhydrazone (**2a**, **2b**) with *n*-butyllithium affords the lithium salt; thermolysis of the salt at 70−80 °C liberates the diazo compound (**4a**, **4b**), which is not isolated, but rather is co-deposited with argon or nitrogen directly onto a cryogenically cooled spectroscopic window to afford the matrix-isolated sample (Scheme 1).

IR Spectroscopy: Generation and Photochemistry of *t*-BuC_5H (1a). Photolysis (λ > 497 nm, 13.5 h, N_2, 10 K) of matrix-isolated 1-diazo-6,6-dimethylhepta-2,4-diyne (**4a**) affords infrared absorption signals that compare favorably to the computed infrared spectrum of triplet *t*-BuC_5H (**1a**) (Figure 2). Infrared spectra were also computed for several other isomers of *t*-BuC_5H (C_9H_{10}), but none agreed with the experimentally observed infrared spectrum (see Supporting Information). Table 1 lists the correspondence between the experimental frequencies and intensities and those calculated for triplet *t*-BuC_5H (**1a**) at the B3LYP/cc-pVTZ level of theory. Several features are worth noting regarding the comparison of experimental and computed spectra: First, the

(17) Broglia, R. A. *Contemp. Phys.* **1998**, *39*, 371–376.
(18) Crljen, Z.; Baranovic, G. *Phys. Rev. Lett.* **2007**, *98*, 116801/116801–116801/116804.
(19) Hori, Y.; Noda, K.; Kobayashi, S.; Taniguchi, H. *Tetrahedron Lett.* **1969**, 3563–3566.
(20) Hauptmann, H. *Tetrahedron* **1976**, *32*, 1293–1297.
(21) Bowling, N. P.; McMahon, R. J. *J. Org. Chem.* **2006**, *71*, 5841–5847.
(22) Sander, W.; Bucher, G.; Wierlacher, S. *Chem. Rev.* **1993**, *93*, 1583–1621.
(23) Wasserman, E. *J. Chem. Phys.* **1965**, *42*, 3739–3740.
(24) Seburg, R. A.; Patterson, E. V.; McMahon, R. J. *J. Am. Chem. Soc.* **2009**, *131*, 9442–9455.
(25) Noro, M.; Koga, N.; Iwamura, H. *J. Am. Chem. Soc.* **1993**, *115*, 4916.
(26) DePinto, J. T.; deProphetis, W. A.; Menke, J. L.; McMahon, R. J. *J. Am. Chem. Soc.* **2007**, *129*, 2308–2315.
(27) DePinto, J. T.; McMahon, R. J. *J. Am. Chem. Soc.* **1993**, *115*, 12573–12574.
(28) Fulara, J.; Freivogel, P.; Forney, D.; Maier, J. P. *J. Chem. Phys.* **1995**, *103*, 8805–8810.
(29) Ball, C. D.; McCarthy, M. C.; Thaddeus, P. *J. Chem. Phys.* **2000**, *112*, 10149–10155.
(30) Bowling, N. P.; Burrmann, N. J.; Halter, R. J.; Hodges, J. A.; McMahon, R. J. *J. Org. Chem.* **2010**, *75*, DOI: 10.1021/jo101125y.

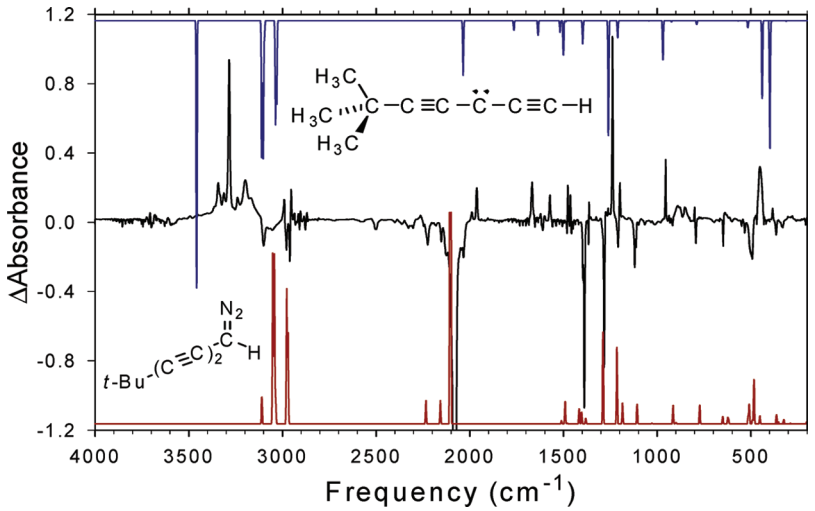

FIGURE 2. Top: Computed IR spectrum of triplet *t*-BuC_5H (**1a**) (B3LYP/cc-pVTZ). Middle: IR subtraction spectrum showing the disappearance of diazo compound **4a** and growth of triplet *t*-BuC_5H (**1a**) upon irradiation ($\lambda > 497$ nm, 13.5 h, N_2, 10 K). Bottom: Computed IR spectrum of diazo compound **4a** (BLYP/6-31G*). The computed intensity of the diazo stretching vibration (2103 cm^{-1}) has been truncated in order to depict the vibrations with lower intensity.

SCHEME 1. Generation of Diazo Compounds and Carbenes

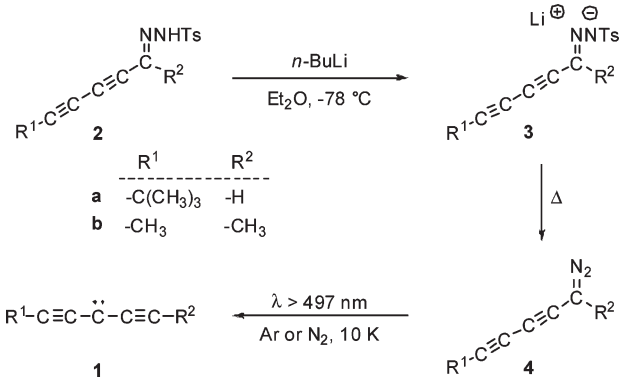

experimental intensities for the bands in the 2868−2992 cm^{-1} range are much lower than expected. These signals belong to C−H stretching modes and coincide strongly with similar bands of diazo compound **4a**; thus, significant cancellation is evident in the subtraction spectrum. Second, a number of peaks not predicted by harmonic analysis appear in the 3150−3350 cm^{-1} region of the spectrum. These bands disappear in concurrence with the other bands assigned to *t*-BuC_5H upon photolysis (see below) and are tentatively assigned to combination modes or overtones. Third, the broad peak at 452 cm^{-1} evidently arises from the overlap of two bending modes of similar frequency (ω_{28}, ω_{29}). Animation of these computed vibrations reveals large-amplitude C≡C−H bending motion for both modes, analogous to vibrations appearing prominently in the IR spectra of matrix-isolated HC_5H[8] and MeC_5H.[9] Apparent overtones or combination bands involving these modes are also found at ca. 850 cm^{-1} here and in the N_2-matrix IR spectra of the previously investigated species.[8,9] Bending at the C≡C−H terminus is believed to be responsible for the vibrational structure observed in the electronic spectra of these species (vide infra).[9]

Irradiation ($\lambda > 399$ nm, 3 h; $\lambda > 363$ nm, 23.1 h; $\lambda > 330$ nm, 108.8 h) of a matrix containing *t*-BuC_5H (**1a**) results in a gradual decrease in intensity of the IR signals ascribed to this species.[31] Disappearance of **1a** is evident after 3 h at $\lambda > 399$ nm, and photolysis proceeds most rapidly when the matrix is irradiated at $\lambda > 330$ nm. Since no photochemistry is observed at longer wavelengths, photolysis of **1a** evidently proceeds via the A^3A_1 state, analogous to MeC_5H[9] (see below). Over the course of the $\lambda > 363$ nm and $\lambda > 330$ nm irradiations, the matrix exhibits visible signs of degradation (i.e., discoloration). In spite of the large amount of *t*-BuC_5H (**1a**) initially present (ca. 1 absorbance unit for the band at 1238 cm^{-1}), the identification of photoproducts by IR spectroscopy is precluded by broad signals and a large number of carbene/photoproduct coincident bands. As will be discussed shortly, changes in the optical spectrum with photolysis exhibit parallels to those for MeC_5H, which undergoes a [1,2]-hydrogen shift when irradiated at these wavelengths.[9]

IR Spectroscopy: Generation and Photochemistry of MeC_5-Me (1b). Considerable difficulty was encountered in obtaining a substantial sample of diazo compound **4b** for infrared spectroscopic experiments. Clean UV/visible and EPR spectra of triplet MeC_5Me (**1b**) were obtained by virtue of the higher sensitivity of these techniques; therefore, our discussion will focus primarily on the results of the latter experiment types.

Photolysis ($\lambda > 497$ nm, 1.5 h, N_2, 10 K) of 2-diazohepta-3,5-diyne (**4b**) results in disappearance of diazo bands and growth of a new set of signals which we assign to triplet MeC_5Me (**1b**, Figure 3). In spite of the low signal intensity, the experimental spectrum in Figure 3 is very clean, and modest agreement is found with the infrared spectrum computed using B3LYP/cc-pVTZ. Experimental and calculated frequencies and intensities are listed in Table 2. The IR spectrum of MeC_5Me exhibits striking resemblance to that of MeC_5H,[9] particularly in the 1000−1800 cm^{-1} range and in the aliphatic C−H stretch region (2800−3000 cm^{-1}).

Extended irradiation into the near-UV ($\lambda > 399$ nm, 2 h; $\lambda > 363$ nm, 19.7 h) results in the simultaneous disappearance of all IR bands ascribed to MeC_5Me (**1b**). A new set of signals appears; these bands remain constant throughout subsequent irradiation cycles to wavelengths as short as 200 nm. Although the carrier(s) of these peaks has not been definitively identified,

(31) Information available as Supporting Information.

TABLE 1. Experimental and Computed Infrared Frequencies and Intensities for Triplet *t*-BuC$_5$H (1a)[a]

B3LYP/cc-pVTZ				expt		B3LYP/cc-pVTZ				expt	
mode	sym	freq	int	freq	int	mode	sym	freq	int	freq	int
ω_1	A_1	3458	131	3283	100	ω_{18}	E	3110	67	2992	11
ω_2	A_1	3102	67	2954	10	ω_{19}	E	3096	9	2935	3
ω_3	A_1	3036	50	2903, 2913	2, 2	ω_{20}	E	3030	40	2868, 2883	2, 1
ω_4	A_1	2035	27	1960	18	ω_{21}	E	1500	17	1464	6
ω_5	A_1	1765	5	1666	24	ω_{22}	E	1489	1		
ω_6	A_1	1636	7	1570	13	ω_{23}	E	1397	11	1363	3
ω_7	A_1	1518	6	1476	9	ω_{24}	E	1210	8	1197	11
ω_8	A_1	1429	0.06			ω_{25}	E	1044	0.1		
ω_9	A_1	1260	56	1238	65	ω_{26}	E	923	1		
ω_{10}	A_1	969	19	954	15	ω_{27}	E	516	3	499	3
ω_{11}	A_1	789	2	798	3	ω_{28}	E	439	38	452	76
ω_{12}	A_1	568	0.1			ω_{29}	E	398	62		
ω_{13}	A_1	312	0.3			ω_{30}	E	386	0.2	383	4
ω_{14}	A_2	3106				ω_{31}	E	330	0.007		
ω_{15}	A_2	1478				ω_{32}	E	267	0.007		
ω_{16}	A_2	969				ω_{33}	E	136	1		
ω_{17}	A_2	211				ω_{34}	E	56	3		

other bands ascribed to *t*-BuC$_5$H (**1a**)

tentative assignment	freq	int
$\omega_1 + \omega_{34}$	3342	22
$2\omega_5$	3313	7
$\omega_5 + \omega_6$	3239	7
$\omega_3 + \omega_{13}$	3197	28
$\omega_{20} + \omega_{13}$	3170	6
$\omega_{11} + \omega_{24}$	1989	4
$2\omega_{28}$ // $2\omega_{29}$ // $\omega_{28} + \omega_{29}$	889, 880, 853	34

[a]Harmonic vibrational frequencies (cm^{-1}) and computed intensities (km/mol). Frequencies have not been scaled. Experimental intensities reported relative to strongest absorption = 100.

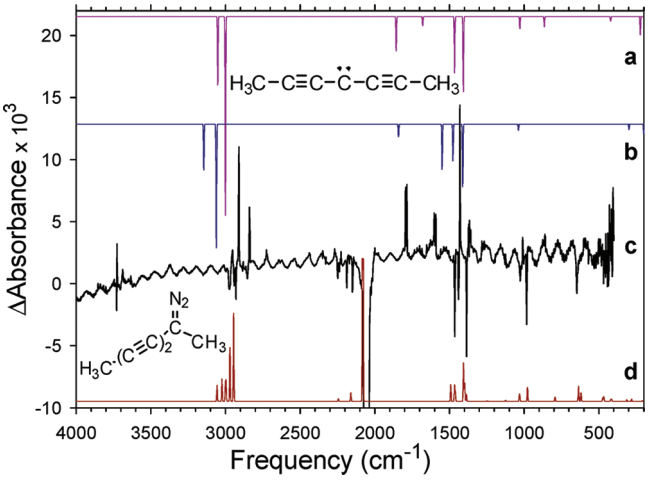

FIGURE 3. (a) Computed IR spectrum of triplet MeC$_5$Me (**1b**) (B3LYP/cc-pVTZ). (b) Computed IR spectrum of triplet MeC$_5$Me (**1b**) (CCSD/cc-pVDZ). (c) IR subtraction spectrum showing the disappearance of diazo compound **4b** and growth of triplet MeC$_5$Me (**1b**) upon irradiation (λ > 497 nm, 1.5 h, N_2, 10 K). The experimental spectrum has been electronically modified to improve signal-to-noise. (d) Computed IR spectrum of 2-diazohepta-3,5-diyne (**4b**) (BLYP/6-31G*). The intensity of the computed diazo stretching vibration (2080 cm^{-1}) has been truncated in order to depict the vibrations with lower intensity.

preliminary results suggest that MeC$_5$Me rearranges to hept-1-ene-3,5-diyne (**5b**) via photochemical [1,2]-hydrogen shift,[31] analogous to MeC$_5$H under similar irradiation conditions.[9]

Electronic Absorption Spectroscopy: Generation and Photochemistry of *t*-BuC$_5$H (1a). Application of the irradiation conditions established in the preceding IR studies of triplet *t*-BuC$_5$H (**1a**) leads to informative changes in the electronic absorption spectra. Figure 4 demonstrates changes that occur in the UV/visible region. Irradiation (λ > 534 nm, 18.2 h; λ > 497 nm, 3 h; λ > 472 nm, 19.5 h; N_2, 13 K) of diazo compound **4a** results in elimination of the intense absorptions below 320 nm and the emergence of several band systems (Figure 4a, solid line). Three absorption patterns are distinguishable: a sharp progression appearing at 220−280 nm (labeled α), a set of broad features in the 280−335 nm range (β), and a system of weak absorptions at 350−430 nm. In a matrix experiment with lower optical density/concentration, it is evident that the α band system is present in the sample prior to irradiation (Figure 4b, dashed line). Photolysis of this sample (λ > 472 nm, 3.1 h, N_2, 10 K) affords the same band systems as before (Figure 4b, solid line), although the intensity ratios differ from the experiment with higher optical density/concentration.

The UV/visible absorption features at 350−430 nm, originating from photolysis of diazo compound **4a** (Figure 4), are virtually identical to those of triplet MeC$_5$H;[9] thus, this progression is unambiguously ascribed to the $A^3A_2 \leftarrow X^3A_2$ absorption of *t*-BuC$_5$H (**1a**). This assignment is supported by observation of the IR spectrum (see above) and EPR spectrum (see below) of triplet *t*-BuC$_5$H (**1a**), as well as the subsequent photochemistry of **1a**, in which the IR, UV/visible, and EPR signals of **1a** decrease upon irradiation into the $A^3A_2 \leftarrow X^3A_2$ absorption (λ > 330 nm).

Extended UV irradiation (λ > 330 nm, 133.5 h) results in the slow depletion of the absorptions of *t*-BuC$_5$H (**1a**) at 350−430 nm, with concomitant growth of the α progression at 220−280 nm (Figure 4b). Plausible photochemical rearrangement pathways of *t*-BuC$_5$H include C−H bond insertion, affording

TABLE 2. Experimental and Computed Infrared Frequencies and Intensities for Triplet MeC_5Me (1b) [a]

		CCSD/cc-pVDZ		B3LYP/cc-pVTZ		expt	
mode	sym	freq	int	freq	int	freq	int
ω_1	A_1'	3056		3000			
ω_2	A_1'	2084		2090			
ω_3	A_1'	1417		1414			
ω_4	A_1'	1157		1172			
ω_5	A_1'	496		504			
ω_6	A_1''	7*i*		13			
ω_7	A_2''	3056	88	3000	102	2910	82
ω_8	A_2''	1837	8	1857	18	1786, 1796	68
ω_9	A_2''	1545	32	1680	5	1590, 1602	43
ω_{10}	A_2''	1409	45	1408	38	1431	100
ω_{11}	A_2''	867	0	866	5	858, 861	11
ω_{12}	E′	3138	33	3051	34	2840	49
ω_{13}	E′	1474	25	1466	28	1359, 1365, 1372	29
ω_{14}	E′	1040	4	1034	6	1009	18
ω_{15}	E′	282	4	421	2		
ω_{16}	E′	194	8	222	10		
ω_{17}	E′	33	10	63	12		
ω_{18}	E″	3138		3051			
ω_{19}	E″	1474		1466			
ω_{20}	E″	1037		1029			
ω_{21}	E″	362		407			
ω_{22}	E″	154		160			

other bands ascribed to MeC_5Me (**1b**)

tentative assignment	freq	int
$\omega_7 + \omega_{17}$ // $\omega_9 + \omega_{13}$	2951	30
$2\omega_{13}$	2726	8

[a] Harmonic vibrational frequencies (cm^{-1}) and computed intensities (km/mol). Frequencies have not been scaled. Experimental intensities reported relative to strongest absorption = 100. Computed structure of D_{3h} symmetry.

1-butadiynyl-2,2-dimethylcyclopropane (**6a**), and 1,2-methyl migration, affording 2,3-dimethylhept-2-ene-4,6-diyne (**5a**) (Scheme 2). The absorptions of the α progression bear a striking resemblance to the spectrum of hex-1-ene-3,5-diyne, the product of photochemical 1,2-hydrogen migration in MeC_5H (Scheme 2).[9] We thus conclude that triplet *t*-BuC_5H (**1a**) undergoes photochemical 1,2-methyl migration to afford 2,3-dimethylhept-2-ene-4,6-diyne (**5a**), which is the carrier the absorptions at 220−280 nm. The fact that the α progression is present as a weak feature in the matrix, prior to irradiation (Figure 4b, dashed line), suggests that a small amount of enediyne **5a** is formed upon thermal decomposition of diazo compound **4a** during the sample deposition process.

The *β* progression in Figure 4 resembles features observed in the electronic spectra of HC_5H[8] and MeC_5H.[9] In the former case, these absorptions were assigned to isomeric $C_{10}H_4$ enediynes (formally, dimers of HC_5H) on the basis of comparison to the electronic spectra of authentic samples.[8,21] Dimerization is believed to be the result of photochemical generation of carbene molecules in the same matrix site, perhaps arising from aggregation of the diazo compound in the vapor phase during sample deposition. Similarities between the features observed in Figure 4 and those in the previous experiments lead us to tentatively assign enediyne dimers of *t*-BuC_5H as the carriers of the *β* progression. This assignment is supported by the observation that the intensity of the *β* progression, relative to that of *t*-BuC_5H, is greater in the "concentrated" matrix than in the "dilute" matrix. The absorption features attributed to *t*-BuC_5H dimers survive the extended UV irradiation ($\lambda > 330$ nm, 133.5 h), which is consistent with the observation that the dimers of HC_5H[8] and

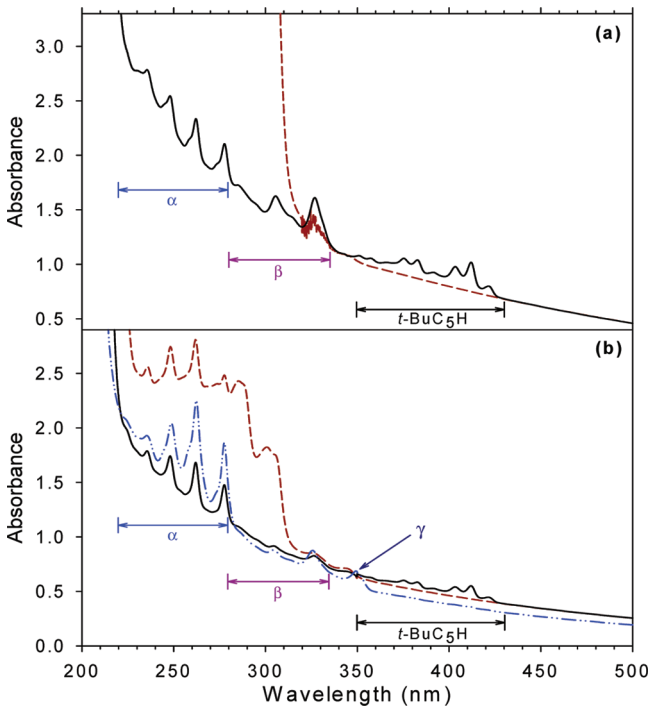

FIGURE 4. Electronic absorption spectra of the generation and photolysis of triplet *t*-BuC_5H (**1a**) in matrices which are initially (a) concentrated and (b) dilute in diazo compound **4a**. In each figure: dashed line, **4a** prior to irradiation; solid line, obtained after complete disappearance of **4a** ($\lambda > 472$ nm); dot-dash line, obtained after complete disappearance of *t*-BuC_5H (**1a**) ($\lambda > 330$ nm).

MeC_5H[9] are photochemically stable under a variety of irradiation conditions. The apparent *growth* of the *β* progression upon irradiation at $\lambda > 330$ nm is not necessarily attributed to formation of additional dimer because of overlap with absorption features associated with the *γ* progression (see below).

Photolysis of *t*-BuC_5H (**1a**) ($\lambda > 330$ nm, 133.5 h) gives rise to additional absorptions near 349 nm (*γ*) (Figure 4b). This feature cannot be assigned to a dimer of *t*-BuC_5H, as it is absent from the dimer progression in the "concentrated" matrix experiment. Given the available data, an assignment for this peak cannot be offered.

Electronic Absorption Spectroscopy: Generation and Photochemistry of MeC_5Me (1b). Application of the irradiation conditions established in the preceding IR studies of triplet MeC_5Me (**1b**) leads to informative changes in the electronic absorption spectra. Figure 5 demonstrates changes that occur in the UV/visible region. Irradiation ($\lambda > 497$ nm, 1.6 h, N_2, 11 K) of 2-diazo-3,5-heptadiyne (**4b**) results in a complete bleaching of the broad absorptions below 320 nm; the resultant spectrum (Figure 5b, black trace) contains a weak set of bands in the 335−415 nm region, characteristic of a triplet $-C_5-$ carbene. This progression is straightforwardly ascribed to the $A^3A_1'' \leftarrow X^3A_2'$ absorption of MeC_5Me (D_{3h} representation). This assignment is supported by observation of the IR spectrum (see above) and EPR spectrum (see below) of triplet MeC_5Me (**1b**), as well as the subsequent photochemistry of **1b**, in which the IR, UV/visible, and EPR signals of **1b** decrease upon irradiation into the $A^3A_1'' \leftarrow X^3A_2'$ absorption ($\lambda > 330$ nm).

Continued UV irradiation ($\lambda > 363$ nm, 31.3 h) effects the disappearance of the absorptions at 335−415 nm and the appearance of sharp bands (α) at 220−280 nm. The observed

SCHEME 2. Carbene Photochemistry

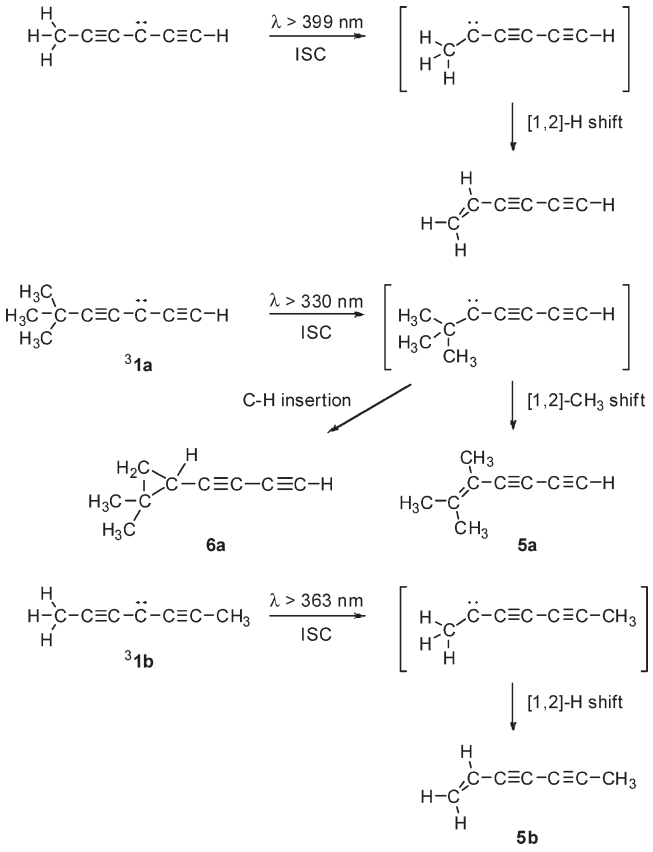

changes are readily interpreted in terms of photoisomerization of triplet MeC_5Me (**1b**) to hept-1-ene-3,5-diyne (**5b**) via [1,2]-hydrogen migration (Scheme 2), in close parallel to the behavior of MeC_5H.[9]

Similar conclusions are drawn from the complementary concentrated matrix experiment presented in Figure 5a. Irradiation ($\lambda > 472$ nm, 3.5 h, N_2, 12 K) depletes the absorptions of the diazo compound from the spectrum, replacing them with the broad features assigned to MeC_5Me (**1b**) at 335−415 nm and several low-intensity peaks in the UV (Figure 5a, black trace). MeC_5Me is completely destroyed by irradiation at $\lambda > 363$ nm for 19.7 h, yielding a spectrum characterized by the prominent α progression at 220−280 nm.

An interesting result of the concentrated matrix experiment is that bands of the α progression can be seen in the spectrum taken following the initial photolysis of the diazo compound. Analogous bands in the spectrum of MeC_5H appeared only after extended irradiation ($\lambda > 363$ nm, 32 h) of the carbene,[9] whereas in the *t*-BuC_5H experiments, a corresponding progression was evident immediately upon deposition. The low intensities of the α system in the black trace of Figure 5a, as compared to the final intensities after carbene photolysis (blue trace), indicate that the carrier is generated from the diazo compound in low yield. Finally, the features appearing at 280−335 nm in the black and blue traces of Figure 5a are assigned to enediyne dimers of MeC_5Me, which are expected to be formed in small quantities in these experiments.

Vibronic Spectra. All alkyl-substituted $R^1-C_5-R^2$ carbenes studied thus far exhibit vibronic progressions in the region of 335−430 nm, analogous to parent HC_5H. The $A^3\Sigma_u^- \leftarrow X^3\Sigma_g^-$ transition of the parent system corresponds to $A^3A_2 \leftarrow X^3A_2$ in C_{3v} symmetry (MeC_5H, *t*-BuC_5H) and $A^3A_1'' \leftarrow X^3A_2'$ in the D_{3h} representation (MeC_5Me). Expansions of the vibronic spectra of **1a** and **1b** obtained in this work are shown in comparison with the spectra of HC_5H,[8] DC_5H,[8] and MeC_5H[9] in Figure 6.

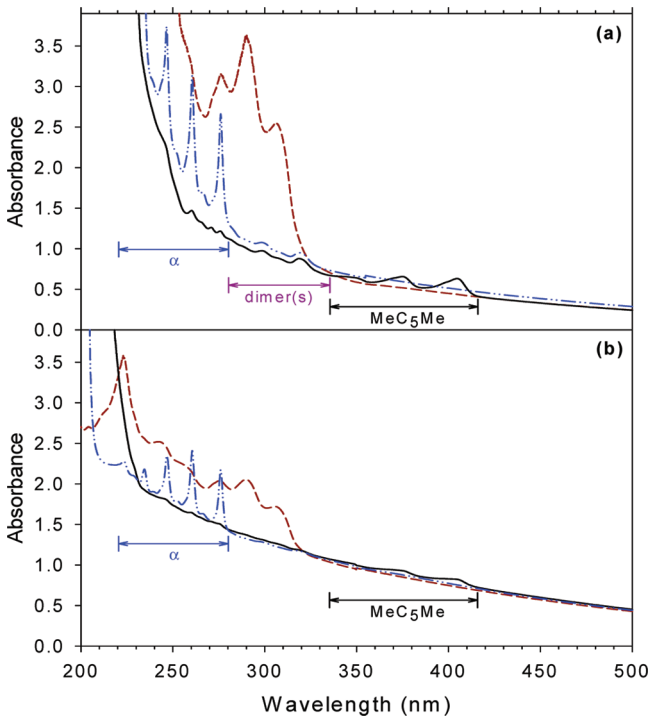

FIGURE 5. Electronic absorption spectra of the generation and photolysis of triplet MeC_5Me (**1b**) in matrices which are initially (a) concentrated and (b) dilute in diazo compound **4b**. In each figure: dashed line, **4b** prior to irradiation; solid line, obtained after complete disappearance of **4b** ($\lambda > 472$ nm); dot-dash line, obtained after complete disappearance of MeC_5Me (**1b**) ($\lambda > 363$ nm).

Although a detailed analysis of the vibronic spectra of these species is the subject of a future publication,[32,33] several features deserve comment. First, the progression of *t*-BuC_5H (**1a**) is virtually identical to that of MeC_5H,[9] demonstrating that the same mechanism is responsible for the vibronic structure in both molecules. In fact, all five species possess band intervals of ~1800−2000 cm^{-1}, intermediate between acetylenic C≡C and allenic C=C stretching frequencies. Calculations predict that parent HC_5H, in the upper $A^3\Sigma_u^-$ state, is bent at both C≡C−H termini, and that the C≡C bonds are elongated.[34] We therefore expect that the $A \leftarrow X$ transitions of these molecules should be accompanied by excitations of C≡C stretching and C≡C−H bending modes. For *t*-BuC_5H (**1a**), this indeed appears to be the case. Although MeC_5Me (**1b**) does not possess a C≡C−H moiety, unresolved vibronic structure can be discerned on the blue side of each band, perhaps accounted for by a lower frequency C≡C−Me bending mode. From Figure 6, we also note that the entire progressions of MeC_5H and *t*-BuC_5H are shifted to the blue of those of HC_5H and DC_5H, while the progression of MeC_5Me appears at even shorter wavelengths.

EPR Spectroscopy: *t*-BuC_5H and MeC_5Me. The triplet EPR spectra of *t*-BuC_5H (**1a**) and MeC_5Me (**1b**) are depicted

(32) Thomas, P. S. Ph.D. Dissertation, University of Wisconsin, 2007.
(33) Thomas, P. S.; McMahon, R. J. Manuscript in preparation.
(34) Stanton, J. F. Unpublished results.

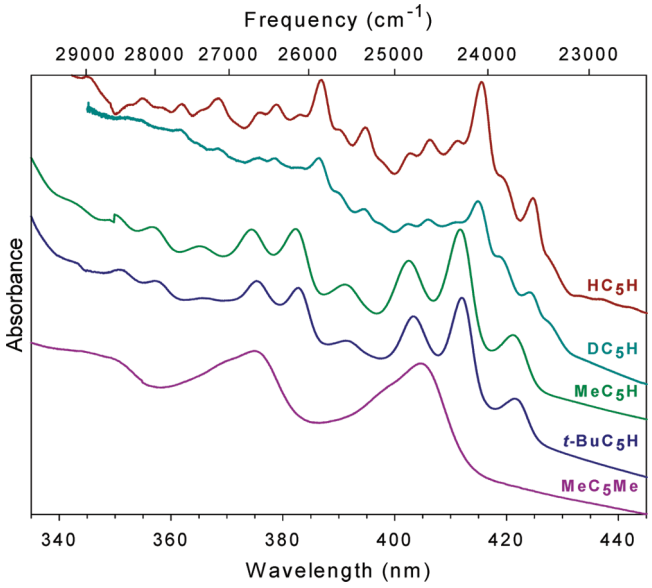

FIGURE 6. Comparison of vibronic features for the $T_1 \leftarrow T_0$ transitions of some $R^1-C_5-R^2$ carbenes. From top to bottom: HC_5H (N_2, 10 K); DC_5H (N_2, 9 K); MeC_5H (N_2, 10 K); *t*-BuC_5H (**1a**, N_2, 13 K); MeC_5Me (**1b**, N_2, 12 K).

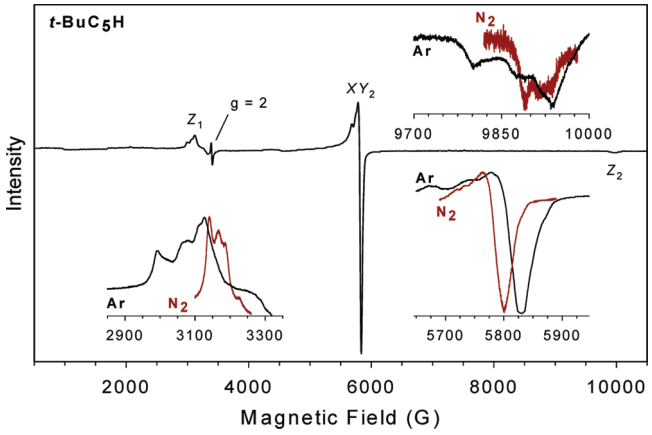

FIGURE 7. X-band EPR spectra of triplet *t*-BuC_5H (**1a**), as generated by photolysis of diazo compound **4a**. Spectra were obtained in argon ($\lambda > 472$ nm, 15 h; 17 K) or in nitrogen ($\lambda > 534$ nm, 17.8 h; $\lambda > 472$ nm, 45.2 h; 15 K). Full spectrum obtained in argon.

in Figures 7 and 8. Values for the transition fields, microwave frequencies, and zero-field splitting (ZFS) parameters for **1a** and **1b** are shown in Table 3. The *D* values for **1a** and **1b** ($|D/hc| = 0.61$ and 0.62 cm^{-1}, respectively) are very similar to those of HC_5H,[8] DC_5H,[8] and MeC_5H,[9−11] as well as that reported previously for *t*-BuC_5H.[10,11] This finding establishes that the alkyl substituents do not significantly perturb the spin density of the unpaired electrons in the π system. Although the *D* value may seem rather large for a species with highly delocalized unpaired spins, it reflects the importance of multiple one-center interactions arising from positive spin density at C-1, C-3, and C-5 and negative spin density at C-2 and C-4 in alkynyl carbenes. This matter is discussed in greater detail elsewhere.[23,24] The very small values of the *E* parameter, which are experimentally indistinguishable from zero, establish that the structures of **1a** and **1b** are axially symmetric (or nearly so). Short-wavelength irradiation of *t*-BuC_5H (**1a**) ($\lambda > 330$ nm) or MeC_5Me

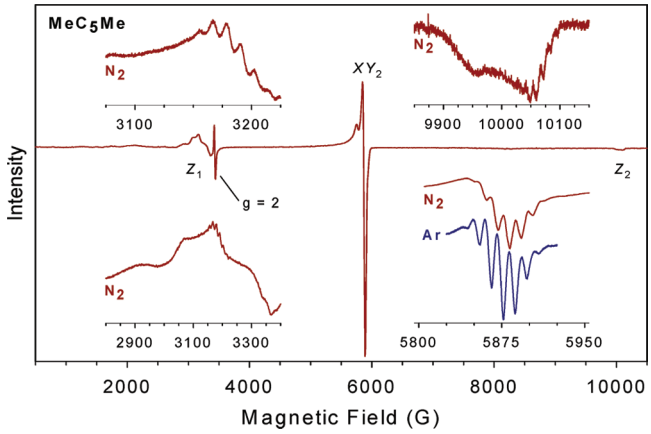

FIGURE 8. X-band EPR spectra of triplet MeC_5Me (**1b**), as generated by photolysis of diazo compound **4b**. Spectra were obtained in argon ($\lambda > 472$ nm, 20.8 h, 16 K) or in nitrogen ($\lambda > 472$ nm, 19.6 h, 16 K). Full spectrum obtained in nitrogen.

TABLE 3. EPR Data for Triplet *t*-BuC_5H (1a) and MeC_5Me (1b)

	t-BuC_5H (**1a**)				MeC_5Me (**1b**)
parameter[a]	Ar	N_2	glass[b]		N_2[c]
Z_1	3128	3166		Z_1	3179
XY_2	5831	5800		X_2	5879
				Y_2	5882
Z_2	9938	9996		Z_2	10060
frequency	9.557	9.480			9.656
$\|D/hc\|$	0.611	0.615	0.6055		0.620
$\|E/hc\|$	0.000	0.000	< 0.0004		0.000

[a]Magnetic field position (G), microwave frequency (GHz), zero-field splitting parameters (cm^{-1}). [b]Poly(chlorotrifluoroethylene), refs 11 and 10. [c]Matrix splittings do not permit reliable assignment of transitions. Peak positions estimated at average positions. Values of zero-field splitting parameters are not sensitive to subtle differences in peak positions (ca. $\pm$ 0.002 cm^{-1}).

(**1b**) ($\lambda > 363$ nm) causes a substantial decrease of the triplet EPR signals in a manner that is consistent with the photochemical transformations observed by IR and UV/vis spectroscopy (see above).[31]

The EPR spectra of *t*-BuC_5H (**1a**) and MeC_5Me (**1b**) are qualitatively similar to those of HC_5H and MeC_5H. The subtle differences that appear upon expanding the regions of the transitions, as previously noted for HC_5H[8] and MeC_5H,[9] also appear for **1a** and **1b**. These differences typically involve small (10−15 G) splittings of the transitions and have been attributed to matrix site effects.[8,9] The XY_2 transition (ca. 5800 G) of *t*-BuC_5H does not exhibit fine structure, while the corresponding transition of MeC_5Me exhibits fine structure in both nitrogen and argon matrices. It has been previously noted that triplet carbenes, obtained from diazo compounds that bear a substituent other than hydrogen at the diazo carbon, typically exhibit fine structure in their EPR transitions arising from nonrelaxed conformations in the matrix.[9] While this behavior is likely to be a factor in describing the spectrum of MeC_5Me (**1b**), we note that splitting effects in matrix EPR spectra may originate from a variety of causes and are difficult to assign with confidence.

Annealing experiments were performed to probe the issues of conformational and matrix effects on the EPR spectra. The experiments were largely inconclusive, however, because instrumental problems restricted our ability to achieve and

SCHEME 3. Oxygen Trapping Chemistry of *t*-BuC$_5$H (1a)[a]

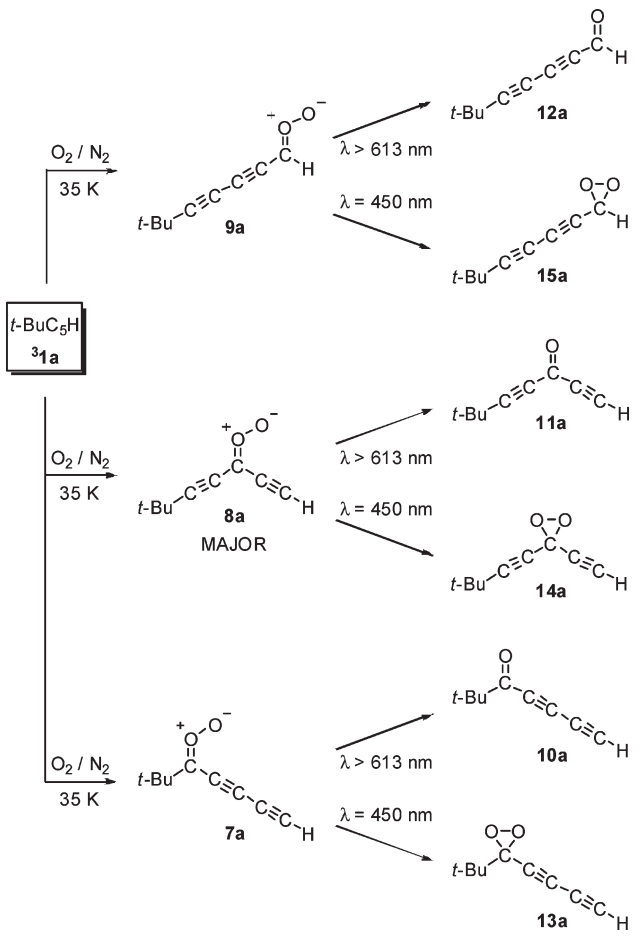

[a]Carbonyl oxides may exist as a mixture of *syn*/*anti* isomers.

maintain temperatures above ca. 30 K. (In previous annealing experiments involving triplet MeC$_5$H, the most significant changes in the EPR spectrum were observed upon warming to 36−41 K.[9]) Annealing a matrix containing triplet *t*-BuC$_5$H (**1a**) (15−30 K, 10 min, N_2), followed by cooling to 16 K, produces very small changes in the Z_1 and XY_2 transitions.[31] Annealing a matrix containing triplet MeC$_5$Me (**1b**) in Ar (26−35 K, 5.5 min) or in N_2 (24−30 K, 5 min), with subsequent cooling to 16 K, results in no changes in the XY_2 region of the spectra.[31] On the basis of the data presented here, the only definitive conclusion that can be drawn is that the triplet carbenes *t*-BuC$_5$H (**1a**) and MeC$_5$Me (**1b**) are thermally stable at temperatures up to 35 K.

Oxygen Trapping of *t*-BuC$_5$H (1a). Most triplet carbenes react readily with O_2 to form carbonyl-(*O*)-oxides, which may then be photochemically converted to dioxiranes and carbonyl products.[22,35,36] The oxygen-trapping chemistry for triplet *t*-BuC$_5$H (**1a**) is summarized in Scheme 3. As in the cases of HC$_5$H[8] and MeC$_5$H,[9] trapping of *t*-BuC$_5$H (**1a**) occurs predominantly at the center carbon in the five-carbon chain to afford the carbonyl oxide **8a** (see below). The subsequent photochemistry of the carbonyl oxide(s) exhibits the characteristic wavelength dependence, affording carbonyl compounds ($\lambda > 613$ nm) or dioxiranes ($\lambda = 450$ nm).

A matrix containing triplet *t*-BuC$_5$H (**1a**) and 0.81% O_2 in N_2 was warmed to 35 K for 10 min to permit diffusion of oxygen through the matrix. Upon annealing, a bright yellow tint was observed on the spectroscopic window, indicative of carbonyl-(*O*)-oxide formation. The infrared subtraction spectrum is consistent with generation of carbonyl-(*O*)-oxide isomers at the expense of carbene **1a**. The prominent features in the IR spectrum of the trapping product(s) (3303, 2211, 2100, 1367 cm^{-1}) are well described in terms of the computed spectra for *syn*/*anti* carbonyl oxide **8a** (Figure 9), which is derived from trapping at the center carbon of the pentadiynylidene chain. The good agreement between experimental and computed spectra leaves no doubt that *syn*/*anti* **8a** represents the major product of the trapping reaction. Although we cannot exclude the possibility that carbonyl oxide **7a** makes a small contribution to the absorption at 3303 cm^{-1} and that carbonyl oxide **9a** makes a small contribution to the absorption at 2211 cm^{-1}, these isomers cannot be more than minor components of the product mixture. The subtraction spectrum of the trapping products, along with computed spectra for all of the isomers of carbonyl-(*O*)-oxides **7a**−**9a**, is presented in the Supporting Information. The photochemistry of the carbonyl oxides is also discussed in detail.

Computational Results. Geometries were optimized and frequencies computed for carbenes **1a** and **1b** under the constraints of axial symmetry. Triplet *t*-BuC$_5$H (**1a**) was restricted to the C_{3v} point group, in which the molecule is found to be a minimum on the potential energy surface using B3LYP/cc-pVTZ (Table 1). The D_{3h} structure of triplet MeC$_5$Me (**1b**) (methyl groups eclipsed) is found to be a minimum on the potential energy surface using B3LYP/cc-pVTZ, while the D_{3h} structure computed using CCSD/cc-pVDZ exhibits one imaginary vibrational mode that corresponds to a low-frequency methyl torsion (7*i* cm^{-1}; Table 2). The D_{3d} structure of **1b** (methyl groups staggered) exhibits an imaginary methyl torsion frequency using either B3LYP/cc-pVTZ (5*i* cm^{-1}) or CCSD/cc-pVDZ (8*i* cm^{-1}). On the basis of the small magnitude of these torsional frequencies, one cannot definitively say whether carbene **1b** is a minimum or a transition state since the curvature of the potential in this coordinate may change sign at a higher level of theory or larger basis set. In any case, the energetic difference between the carbene in staggered and eclipsed conformations is very small.

In Table 4, the computed ground-state structural parameters are shown for triplet carbenes **1a** and **1b** from selected coupled-cluster and density functional calculations. For both species, the computed axial geometry is in accord with EPR measurements. Also relevant are the bond lengths in the carbon skeleton: the structures are predicted to exhibit bond-length alternation between characteristic "long triple bond" (∼1.24−1.26 Å) and "short double bond" (∼1.30−1.31 Å) distances. This effect, well-established in the computational literature[14,16] for linear carbon chains, is a manifestation of the mixture of acetylenic and cumulenic character in the π system.[9,16] As previously noted for HC$_5$H[8] and MeC$_5$H,[9] a larger portion of the spin density is located on the central carbon than either of the terminal carbon atoms,[8,9] an observation that is consistent with the prediction that the C$_1$−C$_2$ bonds are longer than the C$_2$−C$_3$ bonds.

(35) Wierlacher, S.; Sander, W.; Marquardt, C.; Kraka, E.; Cremer, D. *Chem. Phys. Lett.* **1994**, *222*, 319–324.

(36) Sander, W.; Block, K.; Kappert, W.; Kirschfeld, A.; Muthusamy, S.; Schroeder, K.; Sosa, C. P.; Kraka, E.; Cremer, D. *J. Am. Chem. Soc.* **2001**, *123*, 2618–2627.

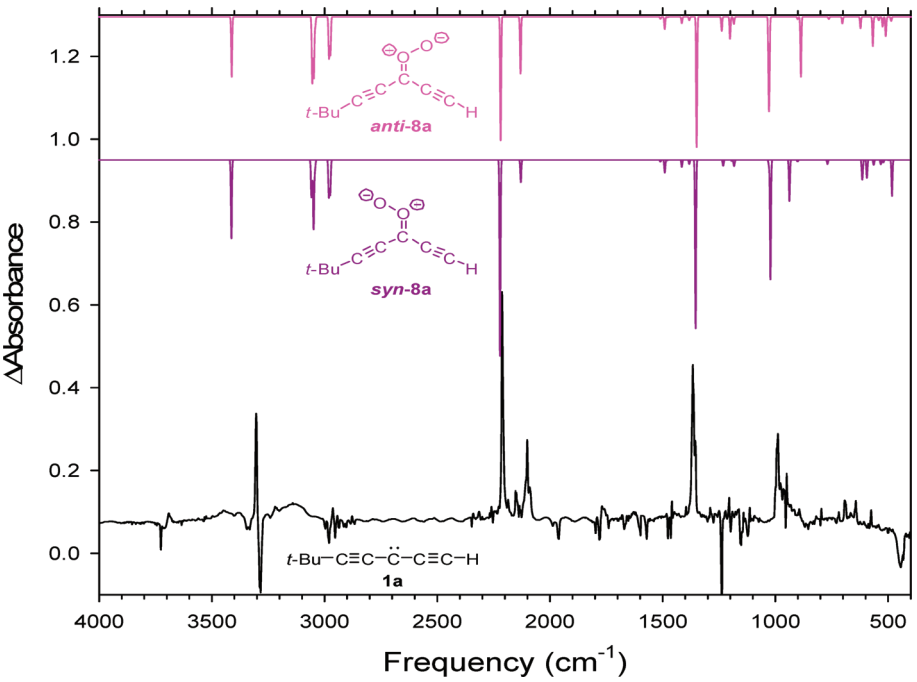

FIGURE 9. Top: Computed IR spectrum of carbonyl oxide *anti*-**8a** (BLYP/6-31G*). Middle: Computed IR spectrum of carbonyl oxide *syn*-**8a** (BLYP/6-31G*). Bottom: IR subtraction spectrum showing the results of annealing an oxygen-doped matrix (0.81% O_2 in N_2) containing *t*-BuC_5H (**1a**) at 35 K (11 min), followed by cooling to 10 K.

TABLE 4. Computed Structural Data for Triplet *t*-BuC_5H (1a) and MeC_5Me (1b)[a]

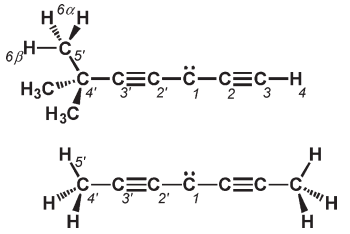

parameter	*t*-BuC_5H (**1a**)[b]	MeC_5Me (**1b**)[b]	MeC_5Me (**1b**)[c]
R (C_1-C_2)	1.3021		
R (C_1-C_2')	1.3035	1.3034	1.3323
R (C_2-C_3)	1.2374		
R ($C_2'-C_3'$)	1.2393	1.2387	1.2561
R (C_3-H_4)	1.0607		
R ($C_3'-C_4'$)	1.4613	1.4476	1.4731
R ($C_4'-H_5'$)		1.0936	1.1048
R ($C_4'-C_5'$)	1.5460		
R ($C_5'-H_{6\alpha}$)	1.0895		
R ($C_5'-H_{6\beta}$)	1.0911		
A ($C_3'-C_4'-H_5'$)		111.302	110.766
A ($C_3'-C_4'-C_5'$)	109.368		
A ($C_4'-C_5'-H_{6\alpha}$)	110.957		
A ($C_4'-C_5'-H_{6\beta}$)	109.716		
D ($C_3'-C_4'-C_5'-H_{6\alpha}$)	±60.202		
D ($C_3'-C_4'-C_5'-H_{6\beta}$)	180		

[a]Bond lengths (Å), bond angles (°). [b]B3LYP/cc-pVTZ. [c]CCSD/cc-pVDZ.

Summary

Triplet carbenes *t*-BuC_5H (**1a**) and MeC_5Me (**1b**) have been investigated by IR, UV/visible, and EPR spectroscopy under matrix-isolation conditions. IR, EPR, and computational data are all consistent with axially symmetric structures for these carbenes. The infrared spectrum of *t*-BuC_5H exhibits features in the C≡C−H bend region (400−900 cm^{-1}) analogous to the spectra of HC_5H[8] and MeC_5H,[9] while MeC_5Me closely resembles MeC_5H[9] in the 1000−1800 cm^{-1} portion of the spectrum. Optical spectra of triplets **1a** and **1b** are characterized by weak transitions with vibrational structure at 335−430 nm, much like the corresponding transitions of HC_5H[8] and MeC_5H.[9] EPR spectra permit the determination of the zero-field splitting parameters, which are very similar in magnitude to previous literature values for HC_5H,[8] MeC_5H,[9−11] and *t*-BuC_5H.[10,11]

Photochemically, *t*-BuC_5H (**1a**) and MeC_5Me (**1b**) behave in a manner which largely parallels that of MeC_5H.[9] IR experiments show that UV irradiation ($\lambda > 399$ nm) of **1a** or **1b** results in their photochemical destruction, as previously reported for MeC_5H.[9] Complementary UV/visible experiments underscore the fact that both *t*-BuC_5H and MeC_5Me rearrange to compounds with π systems similar to 1-hexene-3,5-diyne, the product of MeC_5H photolysis.[9] Finally, computed carbon chain bond lengths of ∼1.24 and ∼1.31 Å are in good agreement with those from computational studies involving other $R^1-C_5-R^2$ molecules.[8,9,13,16] On the basis of both experimental and computational evidence, we conclude that a penta-1,4-diyn-3-ylidene structure ($R^1-C\equiv C-\ddot{C}-C\equiv C-R^2$) represents the dominant contributor to the resonance hybrid, as opposed to the penta-2,4-diyn-1-ylidene structure ($R^1-C\equiv C-C\equiv C-\ddot{C}-R^2$) that was suggested at the time of the early EPR investigations of this family of triplet carbenes.

Methods Section

Experimental Methods. The matrix isolation apparatus and technique have been described previously;[37,38] additional details are provided in the Supporting Information.

(37) McMahon, R. J.; Chapman, O. L.; Hayes, R. A.; Hess, T. C.; Krimmer, H.-P. *J. Am. Chem. Soc.* **1985**, *107*, 7597–7606.
(38) Seburg, R. A.; McMahon, R. J. *J. Am. Chem. Soc.* **1992**, *114*, 7183–7189.

Computational Methods. Equilibrium geometries and harmonic vibrational frequencies calculated using density functional (B3LYP and BLYP) methods utilized the Gaussian 98[39] and Gaussian 03[40] program suites. Equilibrium geometries and harmonic vibrational frequencies calculated using coupled-cluster methods (CCSD) utilized the Mainz-Austin version of the ACESII program.[41]

Generation of Diazo Compounds. The syntheses of tosylhydrazone precursors to diazo compounds **4a** and **4b** are described elsewhere.[30] These tosylhydrazones are stable in a freezer at −20 °C and can be stored for months without significant decomposition. Thermolysis of the corresponding sodium or lithium salts[9] affords the diazo compounds (**4a** or **4b**).

1-Diazo-6,6-dimethylhepta-2,4-diyne (4a). 6,6-Dimethylhepta-2,4-diynal tosylhydrazone (**2a**)[30] (0.1 mmol) is dissolved in diethyl ether and treated with 1 equiv of *n*-BuLi solution (2.29 M in hexanes) at −78 °C. Subsequent warming and removal of solvent under roughing pump vacuum affords the lithium tosylhydrazide salt Li^+**3a**$^-$ as an off-white solid. The flask containing salt Li^+**3a**$^-$ is attached to the matrix-isolation apparatus via glass deposition adapter, and the sample is evacuated at room temperature under diffusion pump vacuum until the pressure reaches $\sim 10^{-7}$ mmHg. Thermolysis of the salt at 68−81 °C, concurrent with N_2 bleed-in (1.2 mmHg/min), results in direct deposition of 1-diazo-6,6-dimethylhepta-2,4-diyne (**4a**) onto a precooled spectroscopic window (21 K). Experience has shown that diazo compound **4a** can be generated by thermolysis of either *syn*- or *anti*-Li^+**3a**$^-$ (or a mixture of both); it is obtained in significantly better yield, however, from the *anti*-isomer.

In the UV/visible experiments, a concentrated sample of 1-diazo-6,6-dimethyl-2,4-heptadiyne (**4a**) was prepared by thermolysis of lithium tosylhydrazide *syn*-Li^+**3a**$^-$ (78 °C, 0.5 h) with N_2 deposition rate of 1.2 mmHg/min (Figure 4a). A dilute sample of **4a** was prepared by thermolysis of lithium tosylhydrazide *syn*-Li^+**3a**$^-$ (75−80 °C, 0.3 h) with N_2 deposition rate of 1.5 mmHg/min (Figure 4b).

An alternative procedure for generating diazo compound **4a** involves formation of the sodium salt of the tosylhydrazone rather than the lithium salt. Treating a stirred solution of 0.16 mmol *anti*-**2a** in CH_2Cl_2 with ∼1 equiv of NaH at room temperature, followed by removal of solvent under vacuum, affords sodium tosylhydrazide *anti*-Na^+**3a**$^-$ as a yellow-white solid. Thermolysis (74−148 °C) of *anti*-Na^+**3a**$^-$ from the reaction flask results in the low-yield trapping of diazo compound **4a** on a coldfinger at 77 K. Since thermolysis of the lithium tosylhydrazide salt *anti*-Li^+**3a**$^-$ proceeds at a lower temperature and in higher yield than the sodium salt, the former protocol is preferred.

2-Diazohepta-3,5-diyne (4b). Dissolution of 0.15 mmol hepta-3,5-diyn-2-one tosylhydrazone (**2b**)[30] (mixture of *syn*- and *anti*-isomers) in diethyl ether, followed by reaction with 1 equiv of *n*-BuLi at −78 °C, results in the formation of lithium tosylhydrazide salt Li^+**3b**$^-$. The salt, which has the appearance of a yellowish solid, is readily obtained by stripping off the solvent under roughing pump vacuum at room temperature. Upon transferring salt Li^+**3b**$^-$ to the matrix-isolation apparatus, direct deposition (75−79 °C, N_2 bleed-in at 1.3 mmHg/min) onto a cold spectroscopic window affords matrix-isolated diazo compound **4b**. This procedure provides a clean sample of **4b** in low yield.

In the UV/visible experiments, a dilute sample of 2-diazohepta-3,5 diyne (**4b**) was prepared by thermolysis of Li^+**3b**$^-$ (0.157 mmol, 75−80 °C, 0.6 h) with N_2 deposition rate of 0.9 mmHg/min (Figure 5b). A more substantial portion of diazo compound **4b** is obtained from thermolysis of Li^+**3b**$^-$ (0.359 mmol, 80−87 °C, 0.5 h) with N_2 deposition rate of 1.3 mmHg/min (Figure 5a).

Acknowledgment. We gratefully acknowledge financial support from the National Science Foundation (CHE-0412707 and CHE-0715305). We also acknowledge NSF support for Departmental facilities used in this research: EPR spectrometer (NSF-9013030), computing facilities (NSF-0091916), and NMR instrumentation (NSF-0342998).

Supporting Information Available: Experimental details concerning the preparation of the tosylhydrazone salts that serve as precursors to diazo compounds **4a** and **4b**; IR data for the photolysis of *t*-BuC_5H (**1a**) and MeC_5Me (**1b**); oxygen-trapping IR experiments for *t*-BuC_5H; UV/visible comparison of photochemistry of *t*-BuC_5H (**1a**) and MeC_5Me (**1b**) to that of MeC_5H; EPR photolysis and annealing data for *t*-BuC_5H (**1a**) and MeC_5Me (**1b**); experimentally observed UV/visible absorptions; experimentally observed IR frequencies and intensities; computed harmonic frequencies and intensities; Cartesian coordinates and energies of equilibrium structures. This material is available free of charge via the Internet at http://pubs.acs.org.

(39) Frisch, M. J.; Trucks, G. W.; Schlegel, H. B.; Scuseria, G. E.; Robb, M. A.; Cheeseman, J. R.; Zakrzewski, V. G.; Montgomery, J. A., Jr.; Stratmann, R. E.; Burant, J. C.; Dapprich, S.; Millam, J. M.; Daniels, A. D.; Kudin, K. N.; Strain, M. C.; Farkas, O.; Tomasi, J.; Barone, V.; Cossi, M.; Cammi, R.; Mennucci, B.; Pomelli, C.; Adamo, C.; Clifford, S.; Ochterski, J.; Petersson, G. A.; Ayala, P. Y.; Cui, Q.; Morokuma, K.; Malick, D. K.; Rabuck, A. D.; Raghavachari, K.; Foresman, J. B.; Cioslowski, J.; Ortiz, J. V.; Stefanov, B. B.; Liu, G.; Liashenko, A.; Piskorz, P.; Komaromi, I.; Gomperts, R.; Martin, R. L.; Fox, D. J.; Keith, T.; Al-Laham, M. A.; Peng, C. Y.; Nanayakkara, A.; Gonzalez, C.; Challacombe, M.; Gill, P. M. W.; Johnson, B.; Chen, W.; Wong, M. W.; Andres, J. L.; Gonzalez, C.; Head-Gordon, M.; Replogle, E. S.; Pople, J. A. *Gaussian 98*, revision A.6; Gaussian, Inc.: Pittsburgh, PA, 1998.

(40) Frisch, M. J.; Trucks, G. W.; Schlegel, H. B.; Scuseria, G. E.; Robb, M. A.; Cheeseman, J. R.; Montgomery, J. A., Jr.; Vreven, T.; Kudin, K. N.; Burant, J. C.; Millam, J. M.; Iyengar, S. S.; Tomasi, J.; Barone, V.; Mennucci, B.; Cossi, M.; Scalmani, G.; Rega, N.; Petersson, G. A.; Nakatsuji, H.; Hada, M.; Ehara, M.; Toyota, K.; Fukuda, R.; Hasegawa, J.; Ishida, M.; Nakajima, T.; Honda, Y.; Kitao, O.; Nakai, H.; Klene, M.; Li, X.; Knox, J. E.; Hratchian, H. P.; Cross, J. B.; Bakken, V.; Adamo, C.; Jaramillo, J.; Gomperts, R.; Stratmann, R. E.; Yazyev, O.; Austin, A. J.; Cammi, R.; Pomelli, C.; Ochterski, J. W.; Ayala, P. Y.; Morokuma, K.; Voth, G. A.; Salvador, P.; Dannenberg, J. J.; Zakrzewski, V. G.; Dapprich, S.; Daniels, A. D.; Strain, M. C.; Farkas, O.; Malick, D. K.; Rabuck, A. D.; Raghavachari, K.; Foresman, J. B.; Ortiz, J. V.; Cui, Q.; Baboul, A. G.; Clifford, S.; Cioslowski, J.; Stefanov, B. B.; Liu, G.; Liashenko, A.; Piskorz, P.; Komaromi, I.; Martin, R. L.; Fox, D. J.; Keith, T.; Al-Laham, M. A.; Peng, C. Y.; Nanayakkara, A.; Challacombe, M.; Gill, P. M. W.; Johnson, B.; Chen, W.; Wong, M. W.; Gonzalez, C.; Pople, J. A. *Gaussian 03*, revision B.05; Gaussian, Inc.: Wallingford, CT, 2004.

(41) Stanton, J. F.; Gauss, J.; Watts, J. D.; Szalay, P. G.; Bartlett, R. J.; Auer, A. A.; Bernholdt, D. E.; Christiansen, O.; Harding, M. E.; Heckert, M.; Heun, O.; Huber, C.; Jonsson, D.; Jusélius, J.; Lauderdale, W. J.; Metzroth, T.; Michauk, C.; Price, D. R.; Ruud, K.; Schiffmann, F.; Tajti, A.; Varner, M. E.; Vázquez, J. ACES II MAB; and the integral packages: MOLECULE (Almlöf, J.; Taylor, P. R.), PROPS (Taylor, P. R.), PROPS and ABACUS (Helgaker, T.; Aa. Jensen, H. J.; Jørgensen, P.; Olsen, J.). Available at: www.aces2.de.